Journal of Materials Chemistry C

Accepted Manuscript

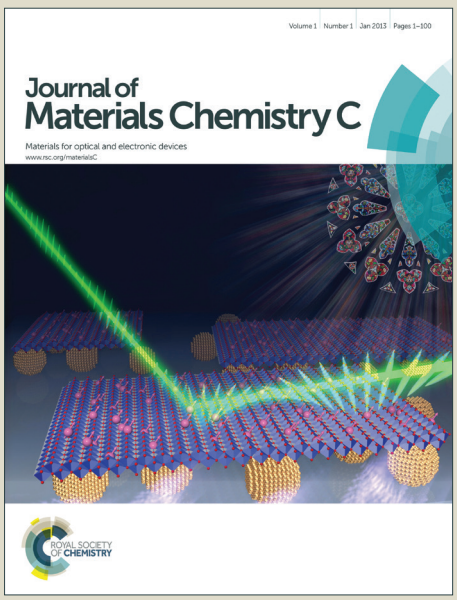

ROYAL SOCIETY OF CHEMISTRY

www.rsc.org/materialsC

Journal Name

RSCPublishing

ARTICLE

Switchable Dielectric Behaviour Associated with Above Room-Temperature Phase Transition in N-Isopropylbenzylammonium Dichloroacetate (N-IPBADC)

Cite this: DOI: 10.1039/x0xx00000x

Received 00th January 2012,
Accepted 00th January 2012

DOI: 10.1039/x0xx00000x

www.rsc.org/

Chengmin Ji,[a] Zhihua Sun,[a,b,c] Shu-Quan Zhang,[a,b] Tianliang Chen,[a] Pan Zhou,[a] Yuanyuan Tang,[a] Sangen Zhao,[a] Junhua Luo[a,b,*]

Bulk transparent single-crystal of N-Isopropylbenzylammonium dichloroacetate (**N-IPBADC**) with sizes of 15×15×10 mm^3, which possesses switchable dielectric permittivities above room-temperature, has been successfully grown by the slow solution cooling method. A reversible second-order solid state phase transition at 366 K was confirmed by thermal analyses including differential scanning calorimetry (DSC) and specific heat (C_p), dielectric measurements, variable-temperature single crystal X-ray diffraction and powder X-ray diffraction (PXRD) analyses. Emphatically, order-disorder transformations of the dichloroacetate moieties in **N-IPBADC** from room temperature phase to high temperature phase have been revealed to induce the distinct dielectric anomaly along with dielectric anisotropic properties above room temperature, up to 366 K. The successful discovering of **N-IPBADC** would potentially pave a new way to explore new above room-temperature phase transition materials.

Introduction Experimental section

The studies on assembling of electronic devices components have been motivated by great interests in applications in data storage, signal processing, sensing, and tunable dielectric devices, etc.[1] The dielectric materials with switchable dielectric behaviour, has long been an important topic to fabricate the electronic devices, which is associated with the reversible electric responses to various external stimulus, such as temperature, electric field, magnetic field, etc.[2] As one of effective strategies, solid-solid phase transition, associated with the reorientational motions of the moieties in the molecules, have recently been utilized to design and synthesize the switchable dielectric materials to study the convertible dielectric behaviour between the striking different dielectric states.[2] In the past two decades, halosceticacids such as difluoroacetic acid, trifluoroacetic acid, dichloroacetic acid and trichloroacetic acid, have been taken as important units to fabricate the phase transition compounds, where the halogen atoms frequently display order–disorder features with the change of ambient temperature, resulting in structure phase transition.[2(b),3] Recently, organic molecule-based switchable dielectrics, which would be environment friendly, easily disposable, and processed at low cost have attracted a great deal of attentions.[4] Up to now, a lot of switchable organic dielectrics has been founded, but mostly with very low phase transition temperatures T_c restricting its application.[4,5] For example, recently, Zhang et al. reported two temperature-induced reversible phase transition compounds, 1,4-Diazoniabicyclo[2.2.2]octane-1-acetate-4-acetic acid chloride trihydrate and its deuterated compound, which exhibit marked switchable dielectric properties between low and high dielectric states at low temperature around 210.7 K and 212.3 K, respectively.[6] Therefore, further exploration of new above room-temperature switchable dielectric materials is strongly imperative to be in favour of its practical application in the electronic technology fields. For instance, Katarzyna et al. reported a dielectric material D-amphetamine sulfate, accompanied with a reversible first-order phase transition at 325 K resulted from the ordering of the $SO4^{2-}$ groups in the molecules.[7] In addition, our group discovered a novel organic chromophore dielectric, 4-N, N-dimethylamino-4'-N-methylstilbazolium trifluoromethanesulfonate, which shows the prominent dielectric response above room-temperature with the phase transition temperature 322 K, enabling it to potentially play a momentous role in electric device applications.[8] However, as far as we know, assembling switchable dielectric materials in artificial crystalline solids, in especial possessing a high phase transition temperature, still is a significant challenge.

In the present work, an above room-temperature switchable dielectric material, N-isopropylbenzylammonium dichloroacetate (abbreviated as **N-IPBADC**), assembled with the building units of N-isopropylbenzylammonium cation and dichloroacetate anions, has been synthesized and characterized.

Bulk crystal with sizes of 15×15×10 mm^3 has been successfully grown with the solution cooling method. The thermal analyses including differential scanning calorimetry

(DSC) and specific heat (C_p), dielectric measurements and single crystal X-ray diffraction analysis have been used to investigate its phase transition. It is noteworthy that **N-IPBADC** possesses an above room-temperature phase transition temperature, up to 366 K, enabling it potentially for the practical applications as smart dielectric materials.

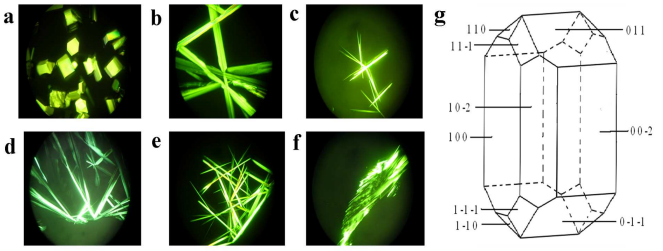

Fig. 1 Photograph of purified micro-crystals from mother solutions of different solvents. The solvents are water, acetonitrile, methanol, ethanol, isopropanol and acetone for images (a)-(f). (g) Morphology of N-IPBADC crystal deduced from BFDH theory.

Experimental section

Usually, bulk high-quality crystals are required for processing and manufacturing dielectric devices. The investigation on crystal morphology crystallized in various solvent is helpful to understand the crystal growth process and significant to optimize the condition for bulk crystal growth. The relative growth rates of various facets of a crystal determine its morphology and the general rule is that slowest growth facets are expressed in the crystal habit.[9] Growth rates of the different crystal facets are influenced by intermolecular interactions between molecules in the crystal and a lot of experimental parameters such as solvent polarity, solvent supersaturation, pH value, temperature, impurities, etc.[10] Fig. 1(a)-(f) show the micro-crystallization photographs of **N-IPBADC** crystals in different solvents. It can be seen clearly that morphology of the crystal becomes more regular in water than those in other solvents and the quality of the crystal could be improved in water. On the contrary, in the solvent of methanol, ethanol, acetone, acetonitrile and isopropanol, the crystalline morphologies of **N-IPBADC** become disorderly acicular and the aggregation phenomenon easily takes place. In acetonitrile, the top crystal faces gradually appear, while with the improvement of the solvents, the crystal morphology becomes cuboid with well-grown prisms in water. As shown in Figure S4, the powder XRD patterns of the microcrystals grown in different solvents match well each other and were in accordance with the simulated pattern based on the room temperature crystal structure, which indicate that all the microcrystals with different morphologies crystallized in various solvents belong to the same space group of $P2_1/c$. Furthermore, its morphology is deduced from BFDH theory, which assumes that the growth rate of a given face is proportional to $1/d_{hkl}$ (d_{hkl} is the interplanar distance of crystal lattice) taking account into symmetry elements, as shown in Figure 1(g).[10,11] The perfect crystal morphology of **N-IPBADC** is a polyhedron with six basal and six top faces, which is analogous to the crystallization morphology in water. Among all the crystal faces, (00−2) and (002) are the most well-developed faces. The dominant faces have also been experimentally confirmed by X-ray diffractions. For the grown

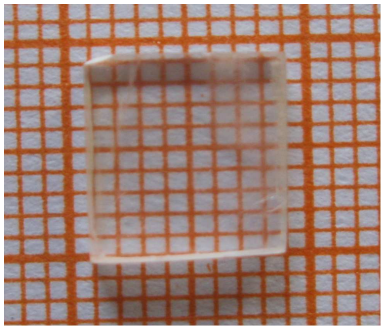

Fig. 2 Photograph of the polished crystal sample of N-IPBADC with dimensions of 10 × 10 × 5 mm^3.

crystal, the largest face is indexed as (00−2) and the adjacent face with (00−2) is indexed as (10-2). As crystal growth progressed, some faces such as (110), (11-1), and (011) often disappear, which may be attributable to the growth environment, such as pH value, temperature field gradient, type of solvent, impurities, etc. The crystal morphology studies and theoretical morphology analyses indicate that it is favorable for the bulk crystal growth in water. All of the starting materials were analytical-grade reagents. The initial materials of **N-IPBADC** were prepared by dissolving N-(1-Methylethyl)-benzenemethanamine and dichloroacetic acid with a molar ratio of 1:1 in deionized water. The solution was stirred and subsequently kept for evaporation at 50 °C for several days. The synthesized salts were purified by successive recrystallization and utilized for growth of **N-IPBADC** crystal. Before starting the crystal growth process, the solution temperature was kept 2 °C above the saturated point for 2-3 h. Then, high optical-quality seed crystals obtained from spontaneous nucleation were used for bulk crystal growth. The temperature was reduced initially at a rate of 0.2 °C/day and subsequently 0.4 °C/day as growth progressed. A colorless and transparent single crystal of size 15 mm × 15mm × 10 mm was obtained in a period of 25 days. Figure 2 presents the as-grown polished sample.

Differential scanning calorimetry (DSC) and specific heat experiments were carried out on a NETZSCH DSC 200 F3 instrument under nitrogen atmosphere in aluminum crucibles with heating and cooling rates of 2 K min^{-1} from 340 K to 380 K (Fig. 3). Dielectric constant measurements were carried out with single crystal samples covered by a silver conductive paste on the surfaces as the electrodes. Complex dielectric permittivities ($\varepsilon = \varepsilon' - i\varepsilon''$) were measured under the frequencies range 10 KHz - 1 MHz with an applied electric field of 0.5 V by using the TH2828A impedance analyzer.

Variable-temperature PXRDs were performed at 298 K, 363 K, 378 K and 383 K on D/MAX2500 Powder X-ray Diffractometer to confirm the phase purity and the reversible structure phase transition of **N-IPBADC**. Variable temperature X-ray single-crystal diffraction data were collected on a Rigaku Saturn 70 diffractometer with Mo-Kα radiation (λ = 0.71073 Å) at 293, 323, 343, 356 and 358 K, respectively. The CrystalClear software package (Rigaku) was used for data collection, cell refinement and data reduction. Crystal structures were solved by the direct methods and refined by the full-matrix method based on F^2 using the *SHELXL* software package.[12] All of the non-hydrogen atoms were refined anisotropically and the positions of the hydrogen atoms were generated geometrically. Crystallographic data and structure refinement of the room temperature phase are listed in Table S1-S3.

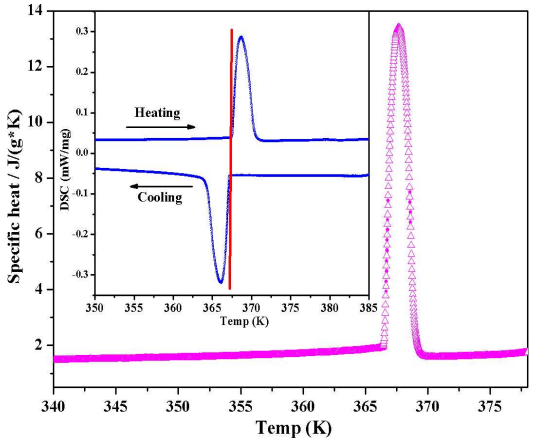

Fig. 3 Curves of specific heat capacity and differential scanning calorimetry of N-IPBADC as a function of temperature.

RESULTS AND DISCUSSION

It is well known that DSC and specific heat (C_p) can be used to effectively detect the existence of a reversible phase transition triggered by temperature. Herein, DSC and specific heat (C_p) measurements of **N-IPBADC** were carried out on the polycrystalline samples and the corresponding traces are shown in Fig. 3. The couple of exothermic and endothermic anomalies represent a reversible phase transition without thermal hysteresis, strongly supporting a continuous character of the transition, being indicative of a second-order phase transition feature.[13] In addition, it has been proved that the C_p-T curves could further confirm an occurrence of phase transition and reveal its characteristic features. As expected, the heat capacity peak of **N-IPBADC** starting at 366 K in the heating mode corresponds well to the DSC (Fig. 3). On the basis of DSC curves, an entropy change (ΔS) accompanying the transition in the heating process is approximately equal to 10.68 J•mol^{-1}•K^{-1}. According to the Boltzmann equation $\Delta S = R\ln N$, where R is the gas constant and N is the ratio of numbers of respective geometrically distinguishable orientations, N is equal to 3.61, strongly suggesting that the phase transition is of the order–disorder type, which may accompany with the reorientations over two equivalent positions of the chlorine atoms in dichloroacetic acid (N = 2).[14] What greatly favors the phase transition of **N-IPBADC** is that the conspicuous thermodynamic phase transformation peak before decomposing in TG/DTA curves. (Figure. S1)

X-ray diffraction analysis of **N-IPBADC** was performed in 293 K. The structure at room temperature phase reveals that the unit cell of the solid-state structure of **N-IPBADC** belongs to the point group of C_{2h}^5 and monoclinic space group $P2_1/c$, with a = 9.700 Å, b = 8.569 Å, c = 17.378 Å, β = 105.8°, where the basic unit is composed a protonated N-Isopropylbenzylammonium cation $(C_{10}H_{16}N)^+$ and an isolated dichloroacetate anion (Cl_2HCCOO^-). The cif file and the detail structural information of **N-IPBADC** are provided in the supporting information. As shown in Fig.4a, there are no disordered atoms at this temperature in the structure unit. Some strong N-H•••O (2.830 Å) hydrogen bonds can be found between the O atoms of the anions (Cl_2HCCOO^-) and the N atoms of the cations $(C_{10}H_{16}N)^+$, resulting in the formation of

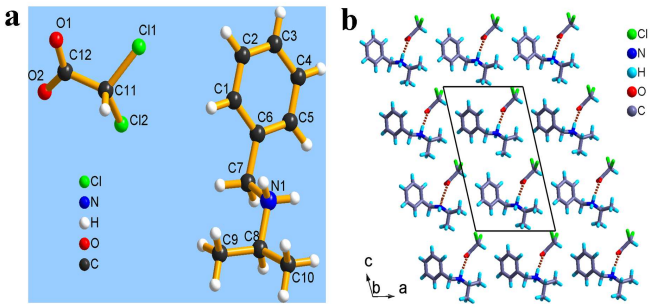

Fig. 4 (a) Molecular structure and (b) Packing diagram of N-IPBADC at room temperature along the b-axis.

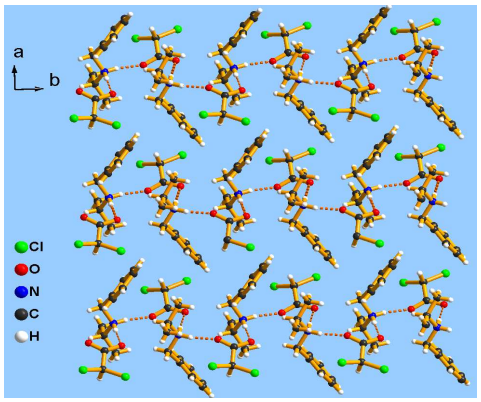

Fig. 5 Packing diagram of N-IPBADC at room temperature along the c-axis.

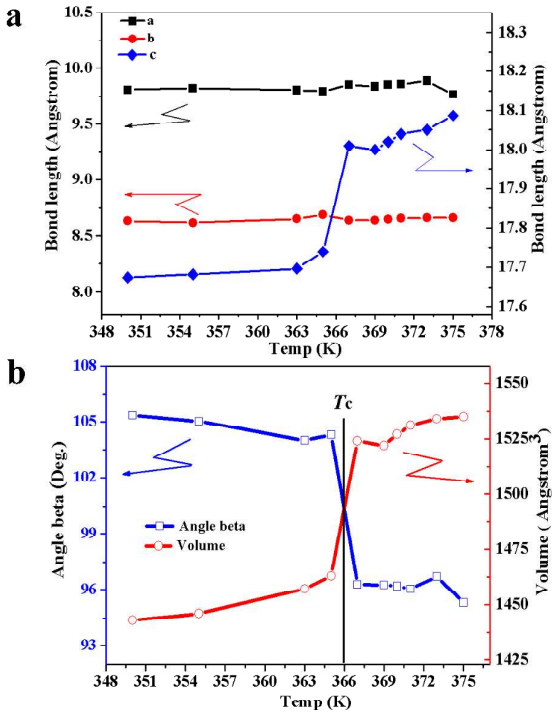

Fig. 6 Temperature dependence of (a) cell parameter changes for three axis lengths and (b) crystal volume and monoclinic β angle in the range from 348 to 385 K of N-IPBADC.

H-bonded dimers as shown in Fig.4b. These dimers in the *a*-*c* plane are then antiparallel to each other along *b* axis related by the 2_1 screw axis parallel to *b via* N-H•••O (2.735 Å) hydrogen bonds, constructing an infinite 1D chain configuration as shown in Figure 5.

Fig.6a and 6b present the unit cell parameters as a function of temperature obtained from single-crystal X-ray measurements between 348 and 385 K, clearly showing that **N-IPBADC** exhibits structural anomalies corresponding to the phase transition detected by differential scanning calorimetry at 366 K. The lattice constants, *a* and *b*, keep a little change between the high temperature phase and room temperature phase. It should be noticed that the lattice constant *c* and the cell volume expand by about 12.7% and 6% at the transition temperature, respectively. Meanwhile the large distortion is characterized by a significant change in the monoclinic β angle, by nearly 10°, which certifies the **N-IPBADC** still belongs to the monoclinic system. The cell parameters of *c* axis, cell volume and monoclinic β angle show abrupt changes at 366 K, revealing a reversible second-order phase transition characteristics, which matches well with the results of the DSC and C_p measurements.

Because it was difficult to obtain a high-temperature phase single-crystal structure of **N-IPBADC** above 366 K, variable-temperature powder X-ray diffraction (PXRD) experiments were performed to reveal the phase transition (Fig. 7). A clear structural phase transition was observed from the PXRD patterns during the warming process. At 363 K (blue line), except the bragg diffractions of (002), (10-2), (11-1), (11-2), (112), (10-4), (21-2), (12-1) and (104) planes of the room temperature phase were observed, some new diffraction peaks appeared, demonstrating the crystal structure phase transition. Especially, the new diffraction peaks marked in pink circle at 9.58°, 10.01°, 17.30°, 18.26°, and 20.21° belong to interim phase, indicating coexistence of the room-temperature phase and high-temperature phase at this temperature. Above 366 K, only diffractions of the high temperature phase were observed. The significant change of diffraction patterns and the cell parameters fairly support the appearance of structure phase transition for **N-IPBADC** at 366 K, which may be triggered by the reorientational motions of the chlorine atoms in dichloroacetate moiety unit.[3b] Furthermore, in order to disclose the origin of the phase transition behaviour, the crystal structures of **N-IPBADC** at 323 K, 343 K, 356 K and 358 K have been measured respectively, which show that the crystal structures are identical below the phase transition temperature

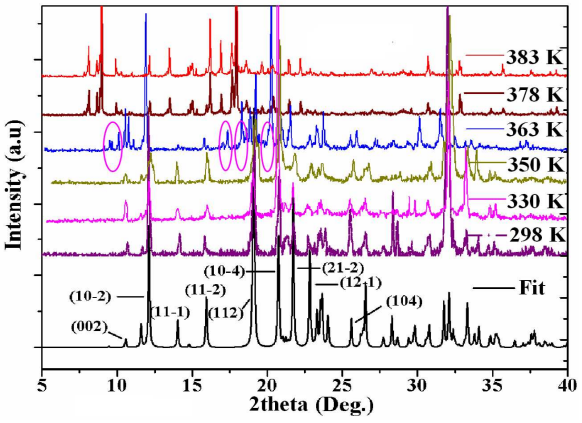

Fig. 7 PXRD patterns of N-IPBADC showing structure phase transition in the temperature range 298–383 K.

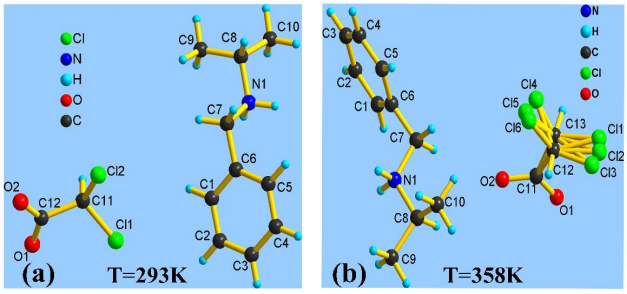

Fig. 8. Structural unit of N-IPBADC in (a) the room temperature phase (293 K) showing ordered dichloroacetate anion, and (b) the high temperature phase (358 K) showing totally disordered dichloroacetate anion.

366 K. (Table S1) However, it is obvious that the thermal vibration parameters U(eq) of the chlorine atoms in dichloroacetate anions increase obviously with temperature increasing.(Table S4) Conclusively, as shown in Figure 8, it is expected that the ordered dichloroacetate anion turns from ordered to disordered at 358 K close to the phase transition temperature due to the severe thermal motions of the chlorine atoms, which results in the structure phase transition for **N-IPBADC** at 366 K.

The distinct anomaly in variable-temperature dielectric response in vicinity of the phase transition point is a strong evidence to discriminate the structural phase transition triggered by the order-disorder change of the chlorine atoms of the dichloroacetate moieties in **N-IPBADC**.[15] The temperature dependence of the real part (ε') and the imaginary part (ε'') of the dielectric constant taken at fixed frequencies of 1 K, 5 K, 10 K, 100 K 500 K and 1MHz over the temperature range from 340 to 380 K are shown in Fig. 9. The dielectric constant remains stable at about 3.4–5 below the T_c of 366 K, and then it displays a pronounced change to high dielectric states with a sharp peak around T_c. A fit of the plot of reciprocal dielectric constant (ε') versus temperature to Curie-Weiss law [$\varepsilon = \varepsilon_\infty + C/(T - T_c)$] gave Curie-Weiss constants C_{HTP} = 23.4 and C_{RTP} = 13.2 for the high temperature phase and room temperature phase, respectively. The C_{HTP}/C_{RTP} ratio of 1.77 is smaller than 4.0, suggesting a second order phase transition.(Figure S3) The imaginary parts of the dielectric constant also display abrupt changes from ca. 0.02.to 0.48 depending on the frequency near the phase transition point as shown in the inset of Fig. 9. Its second-order nonlinear optical (NLO) properties were measured at room temperature and there is no appearance of the second harmonic generation (SHG) signals at 532 nm with 1064 nm laser illumination (Figure S2), indicating that the space group at room temperature phase was exactly the centric $P2_1/c$, which clearly approves that the phase transition is not ferroelectric at 366 K. It is remarkable that the dielectric properties of **N-IPBADC** display sensitive crystal-axis dependence under the same measurement frequency of 10 KHz as shown in Fig. 10. Along the *b*-axis and *c*-axis, the ε' max of the dielectric constant displays the sharp peak and reaches the value of about 15.1 and 10.7 units respectively near the transition temperature. By contrast, only a tiny 'step-like' dielectric anomaly was recorded along the *a*-axis direction. It is noteworthy that such remarkable behaviour of the dielectric anisotropy is similar to that of the typical ferroelectric KDP (KH_2PO_4), which show a tremendous change of sharp peak along the *c*-axis and a tiny 'step-like' change along *a*-axis around the phase transition temperature T_c.[16] The obvious

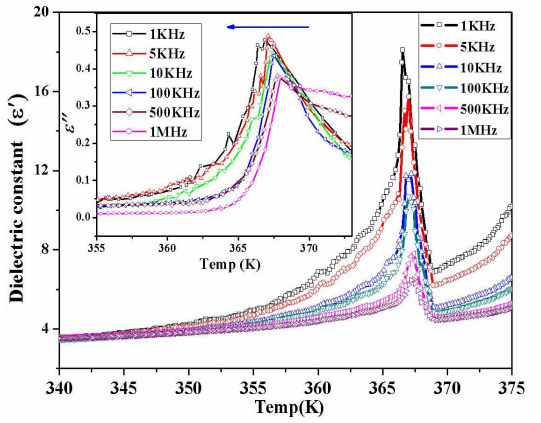

Fig. 9 Temperature dependence of the dielectric response and the imaginary part of the dielectric constant (inset) of N-IPBADC at different frequencies.

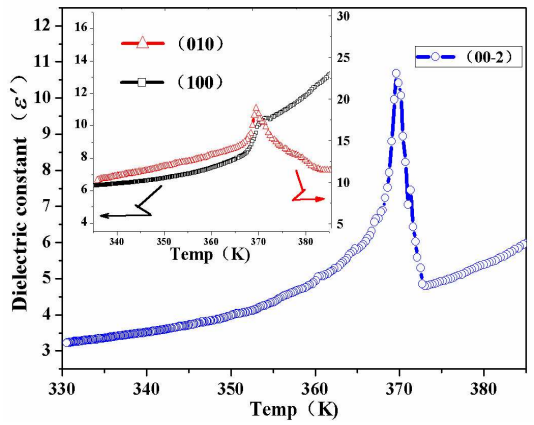

Fig. 10 Anisotropic dielectric response of N-IPBADC along *a, b, c* axis respectively at 10 KHz.

dielectric anisotropy can provide a significant reference for processing crystal and manufacturing dielectric devices. In addition, there is a interesting frequency dispersion behaviour to the dielectric response of **N-IPBADC**, which is more obvious for the imaginary part (ε''), as shown in the inset of Fig. 9, suggesting a "relaxor-like" behaviour at different frequencies, with decreasing frequency, f, the temperature of the peak maximum of imaginary parts, ε'', moves progressively toward lower temperatures. Such a process may be ascribed to the motions of dipolar moments during the order-disorder structure phase transition in **N-IPBADC**, which will be investigated by the forthcoming variable-temperature solid NMR experiments.[2(a), 17]

Conclusions

Bulk optical-quality crystal of **N-IPBADC** with switchable dielectric properties above room-temperature, has been successfully grown using the controlled temperature cooling solution growth technique. It undergoes a reversible second-order phase transition at 366 K verified by the scanning calorimetry (DSC), specific heat (C_p), dielectric measurements, and variable temperature powder X-ray diffraction (PXRD) experiments. The results revealed that the reversible structure phase transition was induced by the ordering-disordering transformations of the chlorine atoms in dichloroacetate moiety units. Importantly, the prominent dielectric anomaly at 366 K makes it to be a promising above room-temperature phase transition material. This successful example may open a useful way to design above room temperature switchable organic dielectric materials.

Acknowledgements

This work was financially supported by the National Nature Science Foundation of China (21222102, 21373220, 51102231, 21171166 and 21301171), the 973 key programs of the MOST (2010CB933501 and 2011CB935904), the One Hundred Talent Program of the Chinese Academy of Sciences and the key project of Fujian Province (2012H0045). Dr. Sun thanks the support from "Chunmiao Project" of Haixi Institute of Chinese Academy of Sciences (CMZX-2013-002).

Notes and references

[a] Key Laboratory of Optoelectronic Materials Chemistry and Physics, Fujian Institute of Research on the Structure of Matter, Chinese Academy of Sciences, Fuzhou, Fujian，350002, P.R. China. E-mail: jhluo@fjirsm.ac.cn. Fax: (+86) 0591483730955. Tel: (+86) 0591483730955.

[b] State Key Laboratory of Structural Chemistry, Fujian Institute of Research on the Structure of Matter, Chinese Academy of Sciences, Fuzhou, Fujian，350002, P.R. China.

[c] State Key Laboratory of Crystal Material, Shandong University, Jinan, 250100, China.

Electronic Supplementary Information (ESI) available: [CIF file, crystal data and structural refinement, atomic coordinates and displacement parameters, bond lengths and angles, TG/DTA curves, CCDC reference numbers 974660 and 987645-987648 for **N-IPBADC** at 293, 323, 343, 356, 358 K.]. See DOI: 10.1039/b000000x/

1 (a) Y. Yu, M. Nakano and T. Ikeda, *Nature*, 2003, **425**, 145; (b) S. H. Baek, H. W. Jang, C. M. Folkman, Y. L. Li, B. Winchester, J. X. Zhang, Q. He, Y. H. Chu, C. T. Nelson, M. S. Rzchowski, X. Q. Pan, R. Ramesh, L. Q. Chen and C. B. Eom, *Nat. Mater*, 2010, **9**, 309; (c) M. Samoc, N. Gautier, M. P. Cifuentes, F. Paul, C. Lapinte and M. G. Humphrey, *Angew. Chem. Int. Ed*, 2006, **45**, 7376.

2 (a) Z. H. Sun, J. H. Luo, S. Q. Zhang, C. M. Ji, L. Zhou, S. H. Li, F. Deng and M. C. Hong, *Adv. Mater*, 2013, **25**, 4159; (b) O. Jeannin, R. Clerac and M. Fourmigué, *J. Am. Chem. Soc*, 2006, **128**, 14649; (c) A. A. Levin and S. P. Dolin, *J. Phys. Chem*, 1996, **100**, 6258; (d) W. Zhang, H. Y. Ye, R. Graf, H. W. Spiess,Y. F. Yao, R. Q. Zhu amd R. G. Xiong, *J. Am. Chem. Soc*, 2013, **135**, 523 0; (e) C. M. Ji, Z. H. Sun, S. Q. Zhang, P. Zhou and J. H. Luo, *J. Mater. Chem. C*, 2014, **2**, 567; (f) W. Zhang, Y. Cai, R-G. Xiong, H. Yoshikawa and K. Awaga, *Angew. Chem. Int. Ed*, 2010, **122**, 6758.

3 (a) S. G. Li, J. H. Luo, Z. H. Sun, S. Q. Zhang, L. N. Li, X. J. Shi and M. C. Hong, *Cryst. Growth. Des*, 2013, **13**, 2675; (b) X. J. Shi, J. H. Luo, Z. H. Sun, S. G. Li, C. M. Ji, L. N. Li, L. Han, S. Q. Zhang, D. Q. Yuan and M. C. Hong, *Cryst. Growth. Des*, 2013, **13**, 2081.

4 (a) J-Z. Ge, X. Q. Fu, T. Hang, Q. Ye and R-G. Xiong, *Cryst. Growth. Des*, 2010, **10**, 3632; (b) D-H. Wu, J-Z. Ge, H-L. Cai, W. Zhang and R-G. Xiong, *CrystEngComm*, 2011, **13**, 319; (c) P. Zhou, Z. H. Sun, S. Q. Zhang, C. M. Ji, S. G. Zhao, R-G. Xiong and J. H. Luo, *J. Mater. Chem. C*, 2014, **2**, 2341; (d) P. Zhou, Z. H. Sun, S. Q.

Zhang, T. L. Chen, C. M. Ji, S. G. Zhao and J. H. Luo. *Chem. Asian J*, 2014, **9**, 996.

5 (a) I. Plowaś,; A. Bialońska, G. Bator, R. Jakubas, W. Medycki and J. Baran, *Eur. J. Inorg. Chem*, 2012, **4**, 636; (b) P. Ciapala, R. Jakubas, G. Bator, J. Zaleski, A. Pietraszko, M. Drozd and J. Baran, *J. Phys. Condens. Matter*, 1997, **9**, 627; (c) L-Z. Chen, H. Zhao, J-Z. Ge, R-G. Xiong and H-W. Hu, *Cryst. Growth. Des*, 2009, **9**, 3828.

6 Y. Zhang, W-Q. Liao, H-Y. Ye, D-W. Fu and R-G. Xiong, *Cryst. Growth. Des*, 2013, **13**, 4025.

7 K. P. Glaser, J. Kaszyńska, A. Rachocki, J. T. Goc, N. Piślewski and A. Pietraszko, *New J. Chem*, 2009, **33**, 1894.

8 Z. H. Sun, J. H. Luo, T. L. Chen, L. N. Li, R-G. Xiong, M-L. Tong and M. C. Hong, *Adv. Funct. Mater*, 2012, **22**, 4855.

9 (a) J. H. Ter Horsta, R. M. Geertmanb and G. M. Van Rosmalena, *J. Cryst. Growth*, 2001, **230**, 277; (b) M. N. Bhat and S. M. Dharmaprakash, *J. Cryst. Growth*, 2002, **242**, 245.

10 T. L. Chen, Z. H. Sun, C. Song, Y. Ge,; J. H. Luo, W. X. Lin and M. C. Hong, *Cryst. Growth Des*, 2012, **5**, 721.

11 (a) A. Bravais, Etudes Crystallographiques; Academie des Sciences: Paris, 1913; (b) G. D. H. Donnay and D. Harker, *Am. Mineral*, 1937, **22**, 446.

12 G. M. Sheldrick, *SHELXL-97*, University of Gottingen, Germany, 1997.

13 (a) Z. H. Sun, X. Q. Wang, J. H. Luo, S. Q. Zhang, D. Q. Yuan and M. C. Hong, *J. Mater. Chem. C*, 2013, **1**, 2561; (b) W. Zhang, H-Y. Ye, H-L. Cai, J-Z. Ge, R-G. Xiong and S. D. Huang, *J. Am. Chem. Soc*, 2010, **132**, 7300.

14 (a) P. Jain, V. Ramachandran, R. J. Clark, H. D. Zhou, B. H. Toby, N. S. Dalal, H. W. Kroto and A. K. Cheetham, *J. Am. Chem. Soc*, 2009, **131**, 13625; (b) P. Jain,; N. S. Dalal, B. H. Toby, H. W. Kroto and A. K. Cheetham, *J. Am. Chem. Soc*,2008, **130**, 10450.

15 (a) S. Horiuchi,; R. Kumai and Y. Okimoto, *J. Am. Chem. Soc*, 1999, **121**, 6757; (b) H-X. Zhao, X-J. Kong, H. Li, Y. C. Jin, L-S. Long, X. C. Zeng, R-B. Huang and L-S. Zheng, *Proc. Natl. Acad. Sci. USA*, 2011, **108**, 3483; (c) Z. H. Sun, T. L. Chen, J. H. Luo and M. C. Hong, *Angew. Chem. Int. Ed*, 2012, **51**, 3871.

16 (a) G. E. Bacon and R. S. Pease, *Proc. Roy. Soc*, London, 1953, **A220**, 397; (b) R. J. Nelmes, V. R. Eiriksson and K. D. Rouse, *Commun. Solid. State. Phys*, 1972, **11**, 1261.

17 (a) D-W. Fu, H-L. Cai, S-H. Li, Q. Ye, L. Zhou, W. Zhang, Y. Zhang, F. Deng and R-G. Xiong, *Phys. Rev. Lett*, 2013, **110**, 257601; (b) M. Hong, *J. Phys. Chem. B*, 2007, **111**, 10340.

Table of Contents

Switchable Dielectric Behaviour Associated with Above Room-Temperature Phase Transition in N-Isopropylbenzylammonium Dichloroacetate (N-IPBADC)

Chengmin Ji,[a] Zhihua Sun,[a,b,c] Shu-Quan Zhang,[a,b] Tianliang Chen,[a] Pan Zhou,[a] Yuanyuan Tang,[a] Sangen Zhao,[a] Junhua Luo[a,b,*]

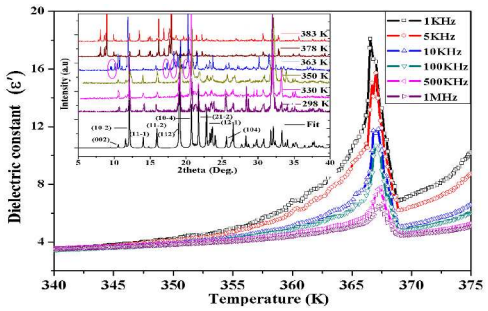

An above-room temperature phase transition material, N-isopropylbenzylammonium dichloroacetate, undergoes a phase transition and exhibits switchable dielectric behaviour around 366 K.